Journal of Sound and Vibration (2000) **234**(5), 819–840
doi:10.1006/jsvi.2000.2897, available online at http://www.idealibrary.com on IDEAL®

ANALYSIS OF FLOQUET WAVE GENERATION AND PROPAGATION IN A PLATE WITH MULTIPLE ARRAYS OF LINE ATTACHMENTS

D. Gueorguiev, J. Gregory McDaniel, P. DuPont and L. B. Felsen†

Department of Aerospace and Mechanical Engineering, Boston University, Boston, MA 02215, U.S.A.

(*Received* 5 *April* 1999, *and in final form* 3 *January* 2000)

A variety of engineering structures consist of a homogeneous "master structure", such as a plate or shell, to which are attached multiple arrays of substructures, such as ribs or stringers. The goal of this work is to understand the effects of array impedance and spacing on energy flow in the master structure. Such an understanding may ultimately lead to a design process encompassing both the attenuation of vibrational energy and the support of static loads. Here, the vibrational response of a locally excited master structure is studied analytically for a class of structures involving an arbitrary number of substructure arrays. The approach is presented in the context of an elastic plate which is reinforced by multiple arrays of line attachments and acted upon by a line force. Extension of the analysis to other geometries and loadings is straightforward. A recursive analytical procedure is presented by which Floquet wavenumbers of a structure with p arrays are computed from the wavenumbers of a structure with $p-1$ of the arrays attached. In this way, the Floquet wavenumbers of any multiple array structure can be computed by first considering the master structure alone and then computing the effect of attaching each array in turn. The imaginary parts of the Floquet wavenumbers quantify the attenuation of response along the structure. In addition, the spatial response is obtained analytically as a sum of two Floquet waves through simplification and transformation of the wavenumber domain solution. By way of example, a three-array structure is considered to illustrate the recursive computation of the wavenumbers and to demonstrate the correlation between the imaginary parts of the wavenumbers and the spatial attenuation of the structural response.

1. INTRODUCTION

Structures such as airplane fuselages and ship hulls are typically subject to mechanical excitations from attached vibrating equipment. These local excitations generate structural waves that radiate noise as they propagate over the structure. The designer typically reduces radiated noise by either positioning resilient mounts between the structure and equipment [1] or by applying various damping treatments to the structure [2]. The former technique attempts to limit the amount of energy transmitted to the structure while the latter attempts to damp the energy after transmission to the structure. Neither technique is ideal and the effectiveness of both techniques usually varies widely as the frequency of excitation is varied.

Another important aspect of structural design involves selecting the locations and designs of multiple substructures such as ribs, stringers, and bulkheads that attach to a master structure, such as a plate or shell. A grouping of identical equally spaced sub-structures shall

† Also department of Electrical and Computer Engineering.

0022-460X/00/300819 + 22 $35.00/0

be referred to here as a sub structure *array*, characterized by its impedance and attachment spacing. While the major structural role of these arrays is to prevent collapse, they may also be designed to control the flow of vibrational energy in the structure.

In order to exploit this control, one must understand the fundamental physics that govern the generation and propagation of Floquet waves in such structures. Floquet waves are waves that naturally propagate in periodic structures and are analogous to the waves that propagate in homogeneous structures. They are best understood by recalling Floquet's theorem for periodic structures, which states that the amplitude of free response, $v(x)$, obeys the identity $v(x) = V(x)\exp(\mathrm{i}k_f x)$, where k_f is the Floquet wavenumber, and $V(x)$ is a spatially dependent wave amplitude that is periodic with the same period as the structure.

The generation of Floquet waves, and in particular the amplitudes of the Floquet waves, is contained in the forced response. The propagation characteristics of these waves are contained in their dispersion relations. The contributions of this paper are to provide, for structures with an arbitrary number of arrays, (1) closed-form expressions for the forced response in terms of Floquet waves and (2) closed-form dispersion relations for the Floquet wavenumbers. Since these results are analytic, they give insight into the effects of array impedance and spacing that could only otherwise be gained through exhaustive numerical studies.

The present work is motivated by the fact that regularly spaced attachments dramatically affect the attenuation of waves in elastic structures. This was first demonstrated by Miles [3], whose work followed Brillouin's observations [4] of "stopping" and "passing" bands experienced by waves in other periodic structures. Miles' analysis of wave propagation in a beam pinned at equally spaced locations involved the solution of a set of difference equations derived by enforcing the boundary conditions at the pinned locations. The resulting equations for the phase and group speeds indicated alternating stop and pass bands. His analysis was extended by Lin [5, 6] to include finite rotational impedances at the pinned locations and by Smith [7] to estimate the coupling of the beam vibrations to an ambient acoustic medium.

Heckl's analysis [8] of plates supported by regularly spaced beams used Ungar's analysis [9] of the reflection and transmission of a flexural wave from a single beam. By accounting for the multiple reflections and transmissions created by regularly spaced beams, equations were derived for the attenuation of flexural waves that also exhibited stop and pass band behavior. Thereafter, analyses of periodic structures have mostly employed two basic analysis methods, both of which assume time-harmonic motions of the structure.

The first method, which shall be referred to here as the *eigenvalue method*, solves an eigenvalue problem for the attenuation constant based on the analysis of one cell of the periodic structure. The eigenvalue problem is derived by applying Floquet's theorem to the responses at the ends of the cell. Applications of Floquet's theorem to the case of a beam with one array of attachments were described by Ungar [10] and Bobrovnitskii and Maslov [11]. Mead [12–15] extended the approach to any linear structure and developed insights into the locations of the stop and pass bands as well as the number of Floquet waves that propagate in a structure. The development of this approach by Mead and others at the University of Southampton is summarized in reference [16].

The second method, which shall be referred to here as the *wavenumber method*, proceeds by taking the spatial Fourier transform of the differential equations of motion of the structure. Once in the wavenumber domain, the structural response is obtained by employing Poisson's summation formula. Each pole of the wavenumber response is known as a Floquet wavenumber and is related to the attenuation constant by a factor of $\sqrt{-1}$.

Upon returning to the spatial domain, the response is found to consist of a linear combination of waves with spatially periodic coefficients. For example, the velocity response of a structure is

$$v(x,t) = \Re\left\{\sum_{n=1}^{N} V_n(x)\exp\left[-\mathrm{i}(\omega t + k_n x)\right]\right\}. \tag{1}$$

The $V_n(x)$ are periodic with the same spatial period as the structure. Early applications of the method are presented by Romanov [17], Evseev [18], and Rumerman [19].

Both methods have been applied to the analysis of structures with two arrays of attachments. The eigenvalue method was employed by Gupta [20]. His analysis revealed the appearance of "minor" stop and pass bands when a second array was added to the structure. His approach was specific to the two-array problem, however, and its extension to a structure with more than two arrays is not obvious. The wavenumber analysis of a plate with two arrays of line attachments was first presented by Mace [21] and was later applied by Burroughs [22] to a cylindrical shell with two arrays of ring attachments. Recently, Cray [23] and Nuttall [24], presented procedures that render explicit expressions for the wavenumber response of a plate with multiple arrays of attachments, each one being arbitrarily shifted with respect to the others. In reference [25], Cray discusses a string supported by offset arrays of attachments and provides explicit solution in the wavenumber domain for the case of two offset arrays. These works have illustrated the complex ways in which sets of arrays interact with each other and the master structure.

This work has also indicated that two arrays can interact with a master structure in ways that dramatically affect the flow of vibrational energy. To better understand the interactions in two-array structures and to develop an understanding of structures with three or more arrays, wavenumber analysis is used here to construct a hierarchical description of the effects of arrays on the spatial attenuation of response in the master structure. Fluid loading is not included in the analysis as our interest lies only in the interactions of the arrays with the master structure and in how these interactions affect the flow of vibrational energy. The results are expected to be valid for fluid-loaded structures when the tractions applied by the ambient fluid medium are much smaller than the dominant vibration-induced stresses in the master structure. For example, this is the case for moderately thick steel structures in air.

The following section defines the class of structures that are considered in the present paper. In sections 3 and 4, we derive the wavenumber domain solutions for the forced response. The solution for the spatial response is then described in section 5. In section 6, we consider an example consisting of a plate with three arrays and demonstrate that the Floquet wave dispersions agree with dispersions predicted by the eigenvalue method. Finally, section 7 presents conclusions and demonstrates that, through modest additional effort, the approach can be generalized to other engineering structures.

2. PROBLEM STATEMENT

Consider a thin elastic plate with P arrays, an example of which is shown in Figure 1. The plate is described by its Young's modulus E, thickness h, mass per unit area m, and the Poisson ratio ν. The midplane of the plate coincides with the xy plane. A harmonic dependence in time and the y co-ordinate is assumed throughout this paper, so that the total force F applied to the plate and its displacement W are represented as

$$F(x,y,t) = \Re\{f(x)\exp[\mathrm{i}(k_y y - \omega t)]\}, \qquad W(x,y,t) = \Re\{w(x)\exp[\mathrm{i}(k_y y - \omega t)]\}. \tag{2, 3}$$

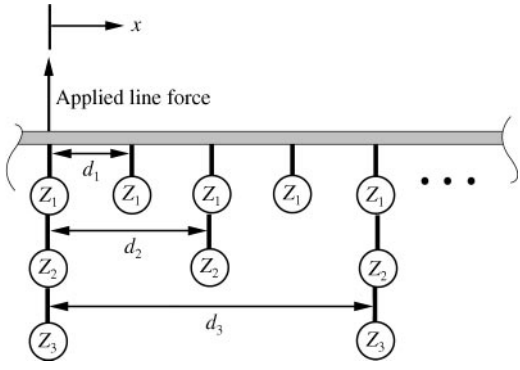

Figure 1. Example structure, consisting of a thin elastic plate with three arrays of line attachments. This particular arrangement is analyzed in section 6. The circles represent line impedances that extend along the y co-ordinate (into page).

Lower-case variables, such as f and w, will generally be used to represent the x-dependent complex amplitude of the corresponding upper-case variables. Henceforth, all dependent variables and attachment impedances will be functions of k_y and ω. This dependence is omitted for brevity.

The equation of motion of the plate with no attachments is

$$D\Delta^2 W - m\frac{\partial^2 W}{\partial t^2} = F, \qquad \Delta^2 = \frac{\partial^4}{\partial x^4} + 2\frac{\partial^4}{\partial x^2 \partial y^2} + \frac{\partial^4}{\partial y^4} \tag{4, 5}$$

and $D = Eh^3/[12(1-\nu^2)]$. Given the assumptions in equations (2) and (3), this equation simplifies to

$$D\left(k_y^4 v - 2k_y^2 \frac{\partial^2 v}{\partial x^2} + \frac{\partial^4 v}{\partial x^4}\right) - m\omega^2 v = -\mathrm{i}\omega f, \tag{6}$$

where the complex amplitude of velocity is given by $v(x) = -\mathrm{i}\omega w(x)$. Hysteretic damping is included in the frequency domain by allowing the Young's modulus to be complex-valued, so that $E = E_0(1 - \mathrm{i}\eta)$ where η is the material loss factor.

Each attachment of each array is assumed to exert a line force on the plate that is linearly proportional to its velocity, the constant of proportionality being the mechanical line impedance Z_p for an attachment in the pth array. An attachment does not exert a moment on the plate. Ordering the arrays such that $d_p > d_{p-1}$, we further require that $d_p = n_p d_{p-1}$, where n_p is an integer. It is also assumed that x locations exists where an attachment from each array interacts with the structure and these locations will be referred to as *points of coincidence*. The origin $x = 0$ is positioned at a point of coincidence. Each array is fully characterized by its spacing d_p and its line impedance Z_p.

The total force applied to the plate is a sum of a unit line force applied at $x = 0$ and the force applied by each attachment of each array,

$$f(x) = \delta(x) - \sum_{p=1}^{p} f_p(x). \tag{7}$$

Each of the f_p terms represents the force applied by the plate to the pth array, which accounts for the minus sign preceding the summation. Each such force is expressed as

$$f_p(x) = Z^{(p)}(x)\, v(x) \quad \text{where } Z^{(p)}(x) = Z_p \sum_{n=-\infty}^{\infty} \delta(x - nd_p). \tag{8}$$

The spatial impedance $Z^{(p)}$ represents the ratio of forces applied by the plate to the velocity at the attachment points.

3. WAVENUMBER DOMAIN FORMULATION

Closed-form expressions for the forced response and Floquet wave dispersion require the solution of equation (4). This shall be accomplished in the wavenumber domain, which is defined by the following Fourier transform pair:

$$\tilde{g}(k) = \int_{-\infty}^{\infty} g(x)\,\mathrm{e}^{-\mathrm{i}kx}\,\mathrm{d}x, \quad g(x) = \frac{1}{2\pi}\int_{-\infty}^{\infty} \tilde{g}(k)\,e^{\mathrm{i}kx}\,\mathrm{d}k, \tag{9, 10}$$

where the symbol " ˜ " over any variable designates the wavenumber transform of that variable throughout this paper. Taking the Fourier transform of equation (4) yields an algebraic relation between the wavenumber velocity $\tilde{v}(k)$ and distributed loading $\tilde{f}(k)$ in terms of the plate admittance $Y(k)$, given by

$$\tilde{v}(k) = \tilde{Y}(k)\tilde{f}(k), \qquad \tilde{Y}(k) = \frac{1}{-\mathrm{i}m\omega}\left[\frac{k_f^4}{k_f^4 - (k^2 + k_y^2)^2}\right]. \tag{11, 12}$$

The wavenumber of flexural waves propagating in the plate without attachments is $k_f = \sqrt[1/4]{m\omega^2/D}$. This wavenumber is complex-valued for a damped plate and real-valued for an undamped plate.

Assuming a unit line force that is independent of k_y, the total force transforms as

$$\tilde{f}(k) = 1 - \sum_{p=1}^{p} \tilde{f}^{(p)}(k), \qquad \tilde{f}^{(p)}(k) = \tilde{Z}^{(p)}(k) * \tilde{v}(k); \tag{13, 14}$$

the symbol " $*$ " designates k-convolution. The Fourier transform of the pth array's impedance is

$$\tilde{Z}^{(p)}(k) = Z_p \sum_{n=-\infty}^{\infty} \exp(-\mathrm{i}knd_p). \tag{15}$$

The convolution indicated in equation (14) may be simplified by Poisson's summation formula. When the general form of Possion's equation, given by (see reference [26, p. 47])

$$\sum_{n=-\infty}^{\infty} g(nd) = \frac{1}{d}\sum_{m=-\infty}^{\infty} \tilde{g}(mk_d) \tag{16}$$

is specialized for the choice $g(x) = \exp(-\mathrm{i}kx)$, we get the identity

$$\sum_{n=-\infty}^{\infty} \exp(-\mathrm{i}knd) = k_d \sum_{n=-\infty}^{\infty} \delta(k - nk_d) \quad \text{where } k_d = 2\pi/d. \tag{17}$$

The identity in equation (17) allows the impedance in equation (15) to be written as

$$\tilde{Z}^{(p)}(k) = k_{d,p} Z_p \sum_{n=-\infty}^{\infty} \delta(k - nk_p) \quad \text{where } k_{d,p} = 2\pi/d_p. \tag{18}$$

Carrying out the convolution indicated in equation (14) gives

$$\tilde{f}^{(p)}(k) = \frac{Z_p}{d_p} \sum_{-\infty}^{\infty} \tilde{v}(k - nk_{d,p}). \tag{19}$$

The wavenumber transform of the total force acting on the plate is then

$$\tilde{f}(k) = 1 - \sum_{p=1}^{p} \frac{Z_p}{d_p} \sum_{n=-\infty}^{\infty} \tilde{v}(k - nk_{d,p}). \tag{20}$$

The wavenumber velocity $\tilde{v}(k)$ now follows from equation (11):

$$\tilde{v}(k) = \tilde{Y}(k) - \tilde{Y}(k) Z_p \sum_{p=1}^{p} \tilde{v}_{\Sigma,p}(k) \tag{21}$$

where

$$\tilde{v}_{\Sigma,p}(k) = \frac{1}{d_p} \sum_{n=-\infty}^{\infty} \tilde{v}(k - nk_{d,p}). \tag{22}$$

The subscript Σ, p on a quantity shall be used to identify a transformed variable, such as $\tilde{v}_{\Sigma,p}(k)$, that is summed over multiples of the pth array wavenumber $k_{d,p}$ and normalized by d_p. Equation (21) represents the coupling of velocity at different wavenumbers due to the different spatial scales of the arrays. The next section presents a method of uncoupling this equation using a generalization of a procedure presented by Mace [21].

4. RESPONSE IN THE WAVENUMBER DOMAIN

To solve equation (21) for the $\tilde{v}(k)$, the spatial scales introduced by the arrays will be successively eliminated. The key concept that allows this elimination is that each $\tilde{v}_{\Sigma,p}(k)$ is periodic in wavenumber with period $k_{p,d}$. The procedure is to find $\tilde{v}_{\Sigma,1}(k)$ in terms of the other $\tilde{v}_{\Sigma,p}(k)$ and $v(k)$ by using the fact that any d_p is an integer multiple of d_1. This allows equation (21) to be written in terms of $\tilde{v}_{\Sigma,p}(k)$, where $p \geqslant 2$, and $v(k)$. Next, the $p = 2$ array is similarly treated. This process, which must begin at $p = 1$ and proceed consecutively to $p = P$, continues until all of the summed velocities are removed from the equation, at which point only $\tilde{v}(k)$ remains. The process will be illustrated here for the $p = 1$ and $p = 2$ arrays and then a general expression for $\tilde{v}(k)$ accounting for all P arrays will be presented.

The analysis is begun by replacing the wavenumber k in equation (21) by the shifted wavenumber $k - qk_{d,1}$, where q is a fixed integer, so as to obtain

$$\tilde{v}(k - qk_{d,1}) = \tilde{Y}(k - qk_{d,1}) - \tilde{Y}(k - qk_{d,1}) \sum_{p=1}^{p} \frac{Z_p}{d_p} \tilde{v}_{\Sigma,p}(k - qk_{d,1}), \tag{23}$$

Since $k_{d,1}$ is an integer multiple of the wavenumbers $k_{d,p}$, the summed velocities $\tilde{v}_{\Sigma,p}(k)$ are periodic with a period of $k_{d,p}$. This observation leads to

$$\tilde{v}_{\Sigma,p}(k - qk_{d,1}) = \frac{1}{d_p} \sum_{n=-\infty}^{\infty} \tilde{v}(k - nk_{d,p} - qk_{d,1}) = \frac{1}{d_p} \sum_{n=-\infty}^{\infty} \tilde{v}(k - (n + qN_p)k_{d,p}), \tag{24}$$

where $N_p = d_p/d_1$ is an integer. This equation involves a shift of the summation index n by the integer amount qN_p and, since the summation is infinite, the following identity holds:

$$\tilde{v}_{\Sigma,p}(k - qk_{d,1}) = \tilde{v}_{\Sigma,p}(k). \tag{25}$$

Summing equation (23) over q from $-\infty$ to ∞, invoking equation (25), and dividing by d_1 yields

$$\tilde{v}_{\Sigma,1}(k) = \tilde{Y}_{\Sigma,1}(k) - \tilde{Y}_{\Sigma,1}(k) \sum_{p=1}^{p} Z_p \tilde{v}_{\Sigma,p}(k), \tag{26}$$

where the notation

$$\tilde{Y}_{\Sigma,1}(k) = \frac{1}{d_1} \sum_{n=-\infty}^{\infty} \tilde{Y}(k - nk_{d,1}) \tag{27}$$

has been introduced for convenience. Rearranging equation (26) allows $\tilde{v}_{\Sigma,1}$ to be expressed in terms of the other velocity sums:

$$\tilde{v}_{\Sigma,1}(k) = \frac{\tilde{Y}_{\Sigma,1}(k)}{1 + Z_1 \tilde{Y}_{\Sigma,1}(k)} - \frac{\tilde{Y}_{\Sigma,1}(k)}{1 + Z_1 \tilde{Y}_{\Sigma,1}(k)} \sum_{p=2}^{p} Z_p \tilde{v}_{\Sigma,p}(k). \tag{28}$$

Substituting equation (28) into equation (21), one obtains $v(k)$ in terms of the summed velocities for the $p > 1$ arrays

$$\tilde{v}(k) = \tilde{Y}_2(k) - \tilde{Y}_2(k) \sum_{p=2}^{p} Z_p \tilde{v}_{\Sigma,p}(k) \tag{29}$$

with the admittance function $\tilde{Y}_2(k)$ defined as

$$\tilde{Y}_2(k) = \frac{\tilde{Y}(k)}{1 + Z_1 \tilde{Y}_{\Sigma,1}(k)}. \tag{30}$$

Physically, $\tilde{Y}_2(k)$ is the wavenumber impedance of the plate with the first array ($p = 1$) attached.

Next, the $p = 2$ array is similarly treated by solving for $\tilde{v}_{\Sigma,2}$ just as we did for $\tilde{v}_{\Sigma,1}$ above. Replacing the wavenumber k in equation (29) by $k - qk_2$, where q is a fixed integer, gives

$$\tilde{v}(k - qk_{d,2}) = \tilde{Y}_2(k - qk_{d,2}) - \tilde{Y}_2(k - qk_{d,2}) \sum_{p=2}^{p} Z_p \tilde{v}_{\Sigma,p}(k - qk_{d,2}). \tag{31}$$

Since $k_{d,2}$ is an integer multiple of $k_{d,p}$, the following identity holds (see equation (25)):

$$\tilde{v}_{\Sigma,p}(k - qk_{d,2}) = \tilde{v}_{\Sigma,p}(k) \quad \text{where } p = 2, \ldots, P. \tag{32}$$

Summing equation (31) over q over from $-\infty$ to ∞, invoking equation (32), and dividing both sides by d_2 yields

$$\tilde{v}_{\Sigma,2}(k) = \tilde{Y}_{\Sigma,2}(k) - \tilde{Y}_{\Sigma,2}(k) \sum_{p=2}^{p} Z_p \tilde{v}_{\Sigma,p}(k) \tag{33}$$

with the second summed admittance defined as

$$\tilde{Y}_{\Sigma,2}(k) = \frac{1}{d_2} \sum_{n=-\infty}^{\infty} \tilde{Y}_2(k - nk_{d,2}). \tag{34}$$

Solving for the summed velocity $\tilde{v}_{\Sigma,2}$ gives

$$\tilde{v}_{\Sigma,2}(k) = \frac{\tilde{Y}_{\Sigma,2}(k)}{1 + Z_2 \tilde{Y}_{\Sigma,2}(k)} - \frac{\tilde{Y}_{\Sigma,2}(k)}{1 + Z_2 \tilde{Y}_{\Sigma,2}(k)} \sum_{p=3}^{p} Z_p \tilde{v}_{\Sigma,p}(k). \tag{35}$$

Substituting equation (35) into equation (29) yields an expression for $\tilde{v}(k)$ that has the same form as equation (29) but with one more summed velocity, $\tilde{v}_{\Sigma,2}$, eliminated to give

$$\tilde{v}(k) = \tilde{Y}_3(k) - \tilde{Y}_3(k) \sum_{p=3}^{p} Z_p \tilde{v}_{\Sigma,p}(k). \tag{36}$$

The admittance wavenumber function $\tilde{Y}_3(k)$ is

$$\tilde{Y}_3(k) = \frac{\tilde{Y}_2(k)}{1 + Z_2 \tilde{Y}_{\Sigma,2}(k)} = \frac{\tilde{Y}(k)}{(1 + Z_1 \tilde{Y}_{\Sigma,1}(k))(1 + Z_2 \tilde{Y}_{\Sigma,2}(k))}, \tag{37}$$

where $\tilde{Y}_{\Sigma,2} = (1/d_2) \sum_{n=-\infty}^{\infty} \tilde{Y}_2(k - nk_{d,2})$.

After performing similar steps until the last unknown quantity $\tilde{v}_{\Sigma,P}$ is eliminated one obtains the following expression for wavenumber velocity

$$\tilde{v}(k) = \frac{\tilde{Y}(k)}{\tilde{Q}(k)}, \tag{38}$$

where $\tilde{Q}(k)$ will be referred to as the *wavenumber dispersion function*. It is periodic in wavenumber with period $k_{d,1}$ and is given explicitly by

$$\tilde{Q}(k) = [1 + Z_1 \tilde{Y}_{\Sigma,1}(k)] [1 + Z_2 \tilde{Y}_{\Sigma,2}(k)] \dots [1 + Z_P \tilde{Y}_{\Sigma,P}(k)]. \tag{39}$$

The summed admittances $\tilde{Y}_{\Sigma,p}$ in equation (39) are defined by

$$\tilde{Y}_{\Sigma,p}(k) = \frac{1}{d_p} \sum_{n=-\infty}^{\infty} \tilde{Y}_p(k - nk_p). \tag{40}$$

They are also periodic in wavenumber with period $k_{d,p}$. In equation (40), $\tilde{Y}_p$ is the wavenumber admittance of the plate with the first $(p-1)$ arrays attached. The pth admittance satisfies the recursion relation

$$\tilde{Y}_p(k) = \begin{cases} \tilde{Y}(k) & \text{if } p = 1, \\ \dfrac{\tilde{Y}_{p-1}(k)}{1 + Z_{p-1} \tilde{Y}_{\Sigma,p-1}(k)} & \text{if } p = 2, \dots, P. \end{cases} \tag{41}$$

Note that the wavenumber velocity of the plate with no attachments is $\tilde{v}(k) = \tilde{Y}(k)$, as one would expect from equation (12) with $\tilde{f} = 1$. The dispersion function $\tilde{Q}(k)$ takes into account the interaction of the plate with all P arrays, and the dispersion relation is simply

$$\tilde{Q}(k) = 0. \tag{42}$$

Note that this result is independent of the inclusion of forcing in equation (7). The above analysis could also be used to show that equation (42) must be satisfied by the unforced system in order to yield a non-trivial solution for the velocity.

One may gain confidence in equations (38) and (39) by considering a structure with P arrays all having the same spacing, d, but each array having an impedance Z_p. For this case, the structure would be behave exactly like a structure with a single array of

attachments with spacing d and with an impedance equal to the sum of the impedances from the P-array structure, $\sum_{p=1}^{P} Z_p$. To show this, one computes the velocity of the P-array structure by evaluating equation (38) and (39) for each array. The velocity of the structure with the first array is

$$\tilde{v}_1(k) = \frac{\tilde{Y}(k)}{1 + Z_1 \tilde{Y}_\Sigma(k)}, \tag{43}$$

where the summed admittance is

$$\tilde{Y}_\Sigma(k) = \frac{1}{d} \sum_{n=-\infty}^{\infty} \tilde{Y}(k - nk_d) \tag{44}$$

and $k_d = 2\pi/d$. Addition of the second array results in a velocity of

$$\tilde{v}_2(k) = \frac{\tilde{Y}(k)}{1 + (Z_1 + Z_2)\tilde{Y}_\Sigma(k)}. \tag{45}$$

This process continues until the velocity of the structure with all P arrays is obtained:

$$\tilde{v}_P(k) = \frac{\tilde{Y}(k)}{1 + \sum_{p=1}^{P} Z_p \tilde{Y}_\Sigma(k)}. \tag{46}$$

Therefore, consecutive application of equations (38) and (39) gives a result which matches the physical expectation that impedances attached to the same position of the structure may be replaced by the sum of the individual impedances.

5. RESPONSE IN THE SPATIAL DOMAIN

In order to return the spatial domain, it is necessary to take the inverse Fourier transform, defined in equation (10), of the velocity $\tilde{v}(k)$ given in equation (38). To do this by contour integration requires determination of the poles of $\tilde{v}(k)$, given by the zeros of $\tilde{Q}(k)$. This can be efficiently performed by first simplifying the function $\tilde{Q}$ after deriving closed-form expressions for each $\tilde{Y}_{\Sigma,p}$. The subsection below presents this derivation followed by contour integration of the simplified $\tilde{Q}$.

5.1. CLOSED-FORM EXPRESSIONS FOR THE SUMMED PLATE ADMITTANCES

The first step of our analysis, namely the finding of $\tilde{Y}_{\Sigma,1}$, follows Mace's analysis [27] of a one-array structure. A new approach is presented here for the finding of $\tilde{Y}_{\Sigma,p}$ where $p > 2$. This approach, which is crucial to the development of closed-form solutions to the multiple-array problem, finds the $\tilde{Y}_{\Sigma,p}$ sequentially, beginning with $p = 1$ and proceeding with higher values of p. In the following treatment, $\tilde{Y}_{\Sigma,1}$ and $\tilde{Y}_{\Sigma,2}$ will be explicitly simplified and the results will be generalized to $\tilde{Y}_{\Sigma,p}$ for any p.

First, the $\tilde{Y}_{\Sigma,1}$ given in equation (27) is rewritten as

$$\tilde{Y}_{\Sigma,1}(k) = \frac{1}{d_1} \sum_{m=-\infty}^{\infty} \tilde{g}_1(mk_{d,1}) \quad \text{where } \tilde{g}_1(u) = \tilde{Y}(k + u) \tag{47}$$

and $\tilde{Y}(k)$ is given in equation (12). Poisson's summation formula, given in equation (16), is evaluated with $d = d_1$ and $g = g_1$ allowing equation (47) to be written as

$$\tilde{Y}_{\Sigma,1}(k) = \sum_{n=-\infty}^{\infty} g_1(nd_1). \tag{48}$$

In order to evaluate equation (48), the spatial function $g_1(x)$ must be found. Taking the inverse transform of $\tilde{g}_1(u)$ gives

$$g_1(x) = \frac{1}{2\pi} \int_{-\infty}^{\infty} e^{ixu} \tilde{Y}(k+u)\, du. \tag{49}$$

Introducing the new variable $\xi = k + u$ into equation (49), we obtain

$$g_1(x) = \frac{e^{-ixk}}{2\pi} \int_{-\infty}^{\infty} e^{ix\xi} \tilde{Y}(\xi)\, d\xi = e^{-ixk} v^{(0)}(x), \tag{50}$$

where

$$v^{(0)}(x) = \frac{1}{2\pi} \int_{-\infty}^{\infty} e^{ix\xi} \tilde{Y}(\xi)\, d\xi \tag{51}$$

is the spatial velocity response of the plate without attachments caused by the applied line force at the origin.

This integral is to be evaluated by contour integration in the complex ξ-plane, which requires determination of the residues of the integrand. The poles of the integrand satisfy the dispersion relation of the plate without attachments:

$$(k^2 + k_y^2)^2 - k_f^4 = 0. \tag{52}$$

This equation has four simple roots, $k = \lambda_i$, where $i = 1, \ldots, 4$, that represent the four simple poles of the integrand in equation (51) given by

$$\lambda_{1,2,3,4} = \pm \sqrt{\pm k_f^2 - k_y^2}. \tag{53}$$

For a damped plate it can be observed that two of the roots lie in the upper half of the complex wavenumber plane, while the other two lie in the lower half-plane, antisymmetric with respect to the first two, as shown in Figure 2. To find $v^{(0)}(x)$, the roots λ_1 and λ_2 are required to lie in the upper half plane and the integration contour given in Figure 2 is used. Applying Jordan's lemma and invoking symmetry considerations in the x-co-ordinate, $v^{(0)}(x)$ is found to be a sum of two waves,

$$v^{(0)}(x) = c_1 e^{i\lambda_1 |x|} + c_2 e^{i\lambda_2 |x|}, \tag{54}$$

with the coefficients c_1 and c_2 given by

$$c_1 = \frac{k_f^2}{4m\omega\lambda_1}, \qquad c_2 = -\frac{k_f^2}{4m\omega\lambda_2}. \tag{55}$$

Substituting equation (50) into equation (48) gives

$$\tilde{Y}_{\Sigma,1}(k) = \sum_{n=-\infty}^{\infty} v^{(0)}(nd_1)\, e^{-ind_1 k}. \tag{56}$$

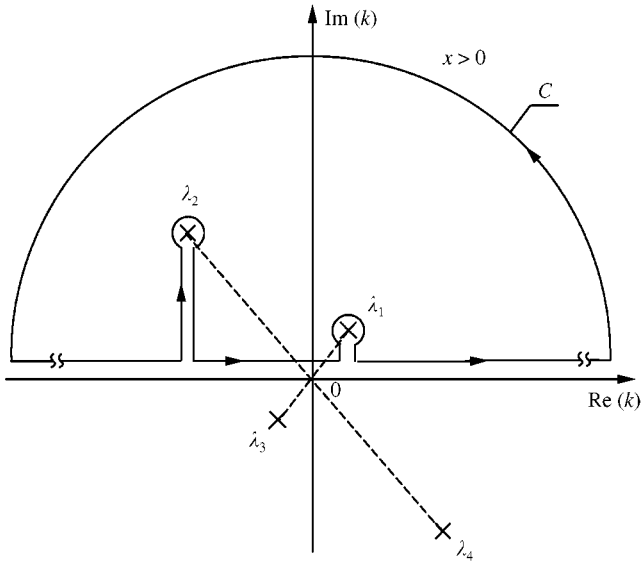

Figure 2. Pictorial representation of the roots of the dispersion relation for a plate with no arrays. The integration contour is also shown.

Evaluating equation (54) at $x = nd_1$ and substituting into equation (56) gives

$$\tilde{Y}_{\Sigma,1}(k) = c_1 \sum_{n=-\infty}^{\infty} e^{-ind_1 k} e^{i\lambda_1 |nd_1|} + c_2 \sum_{n=-\infty}^{\infty} e^{-ind_1 k} e^{i\lambda_2 |nd_1|}. \tag{57}$$

The infinite sums given in equation (57) are evaluated with the aid of the geometric series formula

$$\sum_{n=0}^{\infty} e^{\alpha n d_1} = \frac{1}{1 - e^{\alpha d_1}}, \tag{58}$$

where α is a parameter with $\Re\{\alpha\} < 0$. The first sum in equation (57) reduces to

$$\sum_{n=-\infty}^{\infty} e^{-ind_1 k} e^{i\lambda_1 |nd_1|} = \sum_{n=0}^{\infty} e^{ind_1(\lambda_1 - k)} + \sum_{n=1}^{\infty} e^{ind_1(\lambda_1 + k)}. \tag{59}$$

Identifying $\alpha = \lambda_1 \pm k$ in equation (57) further simplifies this result to

$$\sum_{n=-\infty}^{\infty} e^{-ind_1 k} e^{i\lambda_1 |nd_1|} = \frac{1}{1 - e^{i(\lambda_1 - k)d_1}} + \frac{1}{1 - e^{i(\lambda_1 + k)d_1}} - 1. \tag{60}$$

Using the identities $(e^{-i\lambda d_1} + e^{i\lambda d_1})/2 = \cos(\lambda d_1)$ and $(e^{-i\lambda d_1} - e^{i\lambda d_1})/2 = -i\sin(\lambda d_1)$ with $\lambda = \lambda_{1,2}$ and rearranging, gives

$$\sum_{n=-\infty}^{\infty} e^{-ind_1 k} e^{i\lambda_q |nd_1|} = \frac{-i\sin\lambda_q d_1}{\cos\lambda_q d_1 - \cos k d_1} \quad \text{where } q = 1, 2. \tag{61}$$

Substituting equation (61) into equation (57) yields

$$\tilde{Y}_{\Sigma,1}(k) = A_1 \frac{\sin(\lambda_1 d_1)}{\cos(\lambda_1 d_1) - \cos(k d_1)} + B_1 \frac{\sin(\lambda_2 d_1)}{\cos(\lambda_2 d_1) - \cos(k d_1)}. \tag{62}$$

This expression could also be obtained by applying formula 952 in reference [28].

where the constants A_1 and B_1 are given by

$$A_1 = \frac{k_f^2}{4im\omega\lambda_1} \quad \text{and} \quad B_1 = -\frac{k_f^2}{4im\omega\lambda_2}. \tag{63}$$

Next, the application of this procedure to $Y_{\Sigma,2}$ is summarized. Recall that

$$\tilde{Y}_{\Sigma,2}(k) = \frac{1}{d_2} \sum_{n=-\infty}^{\infty} \tilde{Y}_2(k + nk_{d,2}), \tag{64}$$

where

$$\tilde{Y}_2(k) = \frac{\tilde{Y}(k)}{1 + Z_1 \tilde{Y}_{\Sigma,1}(k)} \quad \text{and} \quad k_{d,2} = \frac{2\pi}{d_2}. \tag{65}$$

As before, $\tilde{Y}_{\Sigma,2}$ is rewritten as

$$\tilde{Y}_{\Sigma,2}(k) = \frac{1}{d_2} \sum_{m=-\infty}^{\infty} \tilde{g}_2(mk_{d,2}) \quad \text{where } \tilde{g}_2(u) = \tilde{Y}_2(k + u). \tag{66}$$

Following the steps in equations (47)–(50) leads to

$$g_2(x) = \frac{e^{-ixk}}{2\pi} \int_{-\infty}^{\infty} \frac{e^{ix\xi} \tilde{Y}(\xi)}{1 + Z_1 \tilde{Y}_{\Sigma,1}(\xi)} d\xi = e^{-ixk} v^{(1)}(x), \tag{67}$$

where

$$v^{(1)}(x) = \frac{1}{2\pi} \int_{-\infty}^{\infty} \frac{e^{ix\xi} \tilde{Y}(\xi)}{1 + Z_1 \tilde{Y}_{\Sigma,1}(\xi)} d\xi \tag{68}$$

is the velocity due to a unit line force acting on the plate with only the $p = 1$ array attached.

To obtain an explicit expression for $v^{(1)}$ by contour integration, we must first determine the zeros of the denominator in the integrand of equation (68). These zeros are given by the roots of

$$1 + Z_1 \tilde{Y}_{\Sigma,1}(k) = 0 \tag{69}$$

which is the dispersion relation for the plate with only the first array attached. This relation has been presented by others (see, for example, reference [10]). Using the closed-form expression for $\tilde{Y}_{\Sigma,1}$ in equation (62), the zeros of equation (69) are found to be the roots of the following quadratic equation in $\cos(kd_1)$:

$$\cos^2(kd_1) + a_1 \cos(kd_1) + b_1 = 0. \tag{70}$$

The coefficients are

$$a_1 = -\cos(\lambda_1 d_1) - \cos(\lambda_2 d_1) - Z_1 \frac{k_f^2}{4im\omega\lambda_1} \sin(\lambda_1 d_1) + Z_1 \frac{k_f^2}{4im\omega\lambda_2} \sin(\lambda_2 d_1), \tag{71}$$

$$b_1 = \cos(\lambda_1 d_1)\cos(\lambda_2 d_1) + Z_1 \frac{k_f^2}{4im\omega\lambda_1} \sin(\lambda_1 d_1)\cos(\lambda_2 d_1)$$

$$- Z_1 \frac{k_f^2}{4im\omega\lambda_2} \sin(\lambda_2 d_1)\cos(\lambda_1 d_1). \tag{72}$$

Equations (70)–(72) agree with the dispersion relation presented by Ungar [9] for a beam with one array of attached impedances.

Let ξ_1 and ξ_2 be the two roots of equation (70). Then the roots that satisfy the dispersion relation (69) are generated by the equations

$$\cos(kd_1) = \xi_{1,2}, \qquad \text{where } \xi_{1,2} = (-a_1 \pm \sqrt{a_1^2 - 4b_1})/2. \tag{73, 74}$$

These roots are repetitive since $\cos(kd_1) = \cos(kd_1 + 2n\pi)$, and they represent simple poles in the integrand of equation (68). There are exactly two roots, $k_1^{(1)}$ and $k_2^{(1)}$, in the strip defined by

$$k_{d,1} > \Re\{k\} \geqslant 0, \quad \text{where } \Im\{(k)\} \geqslant 0. \tag{75}$$

In the present work, this region of the complex wavenumber plane is defined as the *fundamental zone* for the plate with the first array. Accordingly,

$$\cos(k_{1,2}^{(1)} d_1) = \xi_{1,2} \quad \text{where } \frac{2\pi}{d_1} > \Re\{k_{1,2}^{(1)}\} \geqslant 0, \quad \Im\{k_{1,2}^{(1)}\} \geqslant 0. \tag{76}$$

All roots of the dispersion relation equation (69) are given by those in equation (76) subject to the $nk_{d,1}$ shift mentioned earlier.

To calculate $v^{(1)}$ in equation (68), the residue theorem is used with the integration contour given in Figure 3. After applying Jordan's lemma and invoking symmetry in the x-co-ordinate, the spatial velocity $v^{(1)}(x)$ is cast in the form

$$v^{(1)}(x) = 2\pi i \sum_{n=-\infty}^{\infty} \frac{1}{2\pi} \frac{\tilde{Y}(k_1^{(1)} + nk_{d,1})}{Z_1 \tilde{Y}'_{\Sigma,1}(k_1^{(1)} + nk_{d,1})} \exp(k_1^{(1)} + nk_{d,1})|x|) + \text{similar term with } k_2^{(1)}, \tag{77}$$

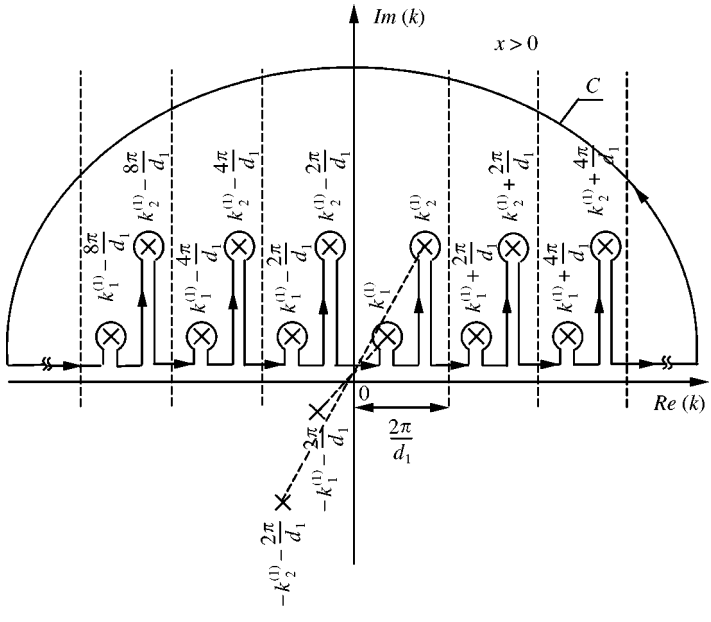

Figure 3. Pictorial representation of the roots of the dispersion relation for a plate with one array of attachments.

where the notation

$$\tilde{Y}'_{\Sigma,1}(k) = \frac{\mathrm{d}\tilde{Y}_{\Sigma,1}(k)}{\mathrm{d}k} \tag{78}$$

has been introduced for convenience.

Upon recognizing that (see equation (62))

$$\tilde{Y}'_{\Sigma,1}(k + nk_{d,1}) = \tilde{Y}'_{\Sigma,1}(k), \tag{79}$$

equation (77) is written as

$$v^{(1)}(x) = W_1^{(1)}(x)\,\mathrm{e}^{\mathrm{i}k_1^{(1)}|x|} + W_2^{(1)}(x)\mathrm{e}^{\mathrm{i}k_2^{(1)}|x|}, \tag{80}$$

where $W_{1,2}^{(1)}(x)$ are periodic functions with period d_1 and are given by

$$W_q^{(1)}(x) = \frac{i}{Z_1\,\tilde{Y}'_{\Sigma,1}(k_q^{(1)})} \sum_{n=-\infty}^{\infty} \tilde{Y}(k_q^{(1)} + nk_{d,1})\,\mathrm{e}^{\mathrm{i}nk_1|x|} \quad \text{where } q = 1, 2. \tag{81}$$

The superscript (1) in equation (81) means that the corresponding quantities are related to the problem where only the first array ($p = 1$) is attached to the plate.

When $x = 0$, one has

$$W_q^{(1)}(0) = \frac{\mathrm{i}d_1\,\tilde{Y}_{\Sigma,1}(k_q^{(1)})}{Z_1\,\tilde{Y}'_{\Sigma,1}(k_q^{(1)})} \quad \text{where } q = 1, 2. \tag{82}$$

Using the Poisson summation formula in equation (16) and $\tilde{g}_2(u) = \tilde{Y}_2(k + u)$ gives

$$\tilde{Y}_{\Sigma,2}(k) = \sum_{n=-\infty}^{\infty} v^{(1)}(nd_2)\,\mathrm{e}^{-\mathrm{i}nd_2k}. \tag{83}$$

Combining equation (80) and (83) and observing that

$$W_q^{(1)}(nd_2) = W_q^{(1)}(nn_2d_1) = W_q^{(1)}(0), \quad q = 1, 2, \quad \text{where } n_2 = \frac{d_2}{d_1}, \tag{84}$$

leads to

$$\tilde{Y}_{\Sigma,2}(k) = W_1^{(1)}(0) \sum_{n=-\infty}^{\infty} \mathrm{e}^{-\mathrm{i}nd_2k}\mathrm{e}^{\mathrm{i}k_1^{(1)}|nd_2|} + W_2^{(1)}(0) \sum_{n=-\infty}^{\infty} \mathrm{e}^{-\mathrm{i}nd_2k}\mathrm{e}^{\mathrm{i}k_2^{(1)}|nd_2|} \tag{85}$$

with the constants $W_{1,2}^{(1)}(0)$ given in equation (82). This is the desired expression for $\tilde{Y}_{\Sigma,2}(k)$.

To obtain a closed-form expression for $\tilde{Y}_{\Sigma,2}$, the infinite sum in equation (85) must be evaluated. Following the procedure of equations (58)–(61) yields

$$\tilde{Y}_{\Sigma,2}(k) = A_2\,\frac{\sin(k_1^{(1)}d_2)}{\cos(k_1^{(1)}d_2) - \cos(kd_2)} + B_2\,\frac{\sin(k_2^{(1)}d_2)}{\cos(k_2^{(1)}d_2) - \cos(kd_2)}, \tag{86}$$

where

$$A_2 = \frac{d_1\,\tilde{Y}_{\Sigma,1}(k_1^{(1)})}{Z_1\,\tilde{Y}'_{\Sigma,1}(k_1^{(1)})}, \qquad B_2 = \frac{d_1\,\tilde{Y}_{\Sigma,1}(k_2^{(1)})}{Z_1\,\tilde{Y}'_{\Sigma,1}(k_2^{(1)})}. \tag{87}$$

Equations (86) and (87), when compared with equations (62) and (63), have a structure that allows generalization to any $Y_{\Sigma,p}$, for $p = 1, 2, \ldots, P$, by induction. Specifically, the results for the pth array are related to those of the $(p-1)$th array. Referring to equations (62) and (86), the summed admittance is written as

$$\tilde{Y}_{\Sigma,p}(k) = A_p \frac{\sin(k_1^{(p-1)} d_p)}{\cos(k_1^{(p-1)} d_p) - \cos(k d_p)} + B_p \frac{\sin(k_2^{(p-1)} d_p)}{\cos(k_2^{(p-1)} d_p) - \cos(k d_p)}, \quad \text{where } p = 2, \ldots, P \tag{88}$$

with the constants A_p and B_p found by induction of equation (87),

$$A_p = \begin{cases} \dfrac{k_f^2}{4\mathrm{i}m\omega\lambda_1} & \text{if } p = 1, \\ \dfrac{d_{p-1}\,\tilde{Y}_{\Sigma,p-1}(k_1^{(p-1)})}{Z_{p-1}\,\tilde{Y}'_{\Sigma,p-1}(k_1^{(p-1)})} & \text{if } p = 2, \ldots, P, \end{cases} \tag{89}$$

$$B_p = \begin{cases} -\dfrac{k_f^2}{4\mathrm{i}m\omega\lambda_2} & \text{if } p = 1, \\ \dfrac{d_{p-1}\,\tilde{Y}_{\Sigma,p-1}(k_2^{(p-1)})}{Z_{p-1}\,\tilde{Y}'_{\Sigma,p-1}(k_2^{(p-1)})} & \text{if } p = 2, \ldots, P. \end{cases} \tag{90}$$

The $k_{1,2}^{p-1}$ are the two Floquet wavenumbers of the plate with the first $p-1$ arrays attached. They lie in the fundamental zone $\Re\{k\} > (2\pi/d_{p-1})$ and $\Im\{k\} \geqslant 0$ and they are simple poles of the dispersion equation, where

$$\tilde{Q}(k) = [1 + Z_1 \tilde{Y}_{\Sigma,1}(k)]\,[1 + Z_2 \tilde{Y}_{\Sigma,2}(k)] \ldots [1 + Z_p \tilde{Y}_{\Sigma,p}(k)]. \tag{91}$$

To justify the above, we refer to equation (69)–(75). The generalization of equation (69) is given by

$$1 + Z_p \tilde{Y}_{\Sigma,p}(k) = 0. \tag{92}$$

5.2. GENERAL RECURSIVE DISPERSIONS RELATIONS

The zeros of equation (92) are the roots of the following quadratic equation with respect to $\cos(k d_p)$ (compare with equations (69)–(75)):

$$\cos^2(k d_p) + a_p \cos(k d_p) + b_p = 0. \tag{93}$$

The values of k that satisfy this equation are the Floquet wavenumbers of the waves that propagate in the structure with p arrays. The coefficients a_p and b_p, which are obtained using the closed-form expression for $\tilde{Y}_{\Sigma,p}$ from the previous step, are given by

$$a_p = -\cos(k_1^{(p-1)} d_p) - \cos(k_2^{(p-1)} d_p) - Z_p A_p \sin(k_1^{(p-1)} d_p) - Z_p B_p \sin(k_2^{(p-1)} d_p), \tag{94}$$

$$b_p = \cos(k_1^{(p-1)} d_p)\cos(k_2^{(p-1)} d_p) + Z_p A_p \sin(k_1^{(p-1)} d_p)\cos(k_2^{(p-1)} d_p) + Z_p B_p \sin(k_2^{(p-1)} d_p)\cos(k_1^{(p-1)} d_p). \tag{95}$$

Then from equations (88) and (93),

$$1 + Z_p \tilde{Y}_{\Sigma,p}(k) = \frac{[\cos(kd_p) - \cos(k_1^{(p)} d_p)]\,[\cos(kd_p) - \cos(k_2^{(p)} d_p)]}{[\cos(kd_p) - \cos(k_1^{(p-1)} d_p)]\,[\cos(kd_p) - \cos(k_2^{(p-1)} d_p)]}. \tag{96}$$

Using equation (96) recursively for $p = 1, 2, \ldots P$, $\tilde{Q}$ will acquire the form

$$\tilde{Q}(k) = \frac{[\cos(kd_p) - \cos(k_1^{(p)} d_p)]\,[\cos(kd_p) - \cos(k_2^{(p)} d_p)]}{[\cos(kd_1) - \cos(\lambda_1 d_1)]\,[\cos(kd_1) - \cos(\lambda_2 d_1)]}, \tag{97}$$

which is useful for inversion to the spatial domain.

5.3. INVERSION OF THE RESPONSE TO THE SPATIAL DOMAIN

Using the closed-form expressions in equation (97) with $p = P$, the dispersion function $\tilde{Q}(k)$ is

$$\tilde{Q}(k) = \frac{\Phi(k)}{\Psi(k)}, \tag{98}$$

where $\Phi(k)$ and $\Psi(k)$ are

$$\Phi(k) = [\cos(kd_P) - \cos(k_1^{(P)} d_P)]\,[\cos(kd_P) - \cos(k_2^{(P)} d_P)], \tag{99}$$

$$\Psi(k) = [\cos(kd_1) - \cos(\lambda_1 d_1]\,[\cos(kd_1) - \cos(\lambda_2 d_1)]. \tag{100}$$

Here, $k_{1,2}^{(P)}$ are the Floquet wavenumbers of the plate with all P arrays attached and they are computed using equation (93) with $p = P$. Since the quadratic equation (93) has recursive coefficients, then in order to obtain the Floquet wavenumbers of the P-array problem, we have to compute first the wavenumbers $k_{1,2}^{(1)}$, then $k_{1,2}^{(2)}$ and so on until $k_{1,2}^{(P)}$. In this way, we adjust the wavenumbers as each array is added to the structure.

To evaluate the spatial velocity $v(x)$ by Fourier inversion (see equation (10)), the residue theorem is applied to the wavenumber velocity of the P-array problem whose velocity in the wavenumber domain is

$$\tilde{v}(k) = \frac{\tilde{Y}(k)}{\tilde{Q}(k)}. \tag{101}$$

The deformed integration contour is shown in Figure 4.

Using Jordan's lemma, recalling that all poles are simple, and taking into account the physical symmetry in the x-co-ordinate gives

$$v(x) = \sum_{r=1}^{2} \sum_{n=-\infty}^{\infty} \mathrm{i}\, \frac{\Psi(k_r^{(P)} + nk_{d,P})\, \tilde{Y}(k_r^{(P)} + nk_{d,P})}{\Phi'(k_r^{(P)} + nk_{d,P})} \exp[(k_r^{(P)} + nk_{d,P})\,|x|], \tag{102}$$

where $\Phi'(k) \equiv \mathrm{d}\Phi/\mathrm{d}k$. Since

$$\Phi'\left(k + \frac{2\pi n}{d_P}\right) = \Phi'(k), \tag{103}$$

the spatial velocity of the above multiple array problem can be cast in the form

$$v(x) = W_1(x)\, \mathrm{e}^{\mathrm{i}k_1^{(p)}|x|} + W_2(x) \mathrm{e}^{\mathrm{i}k_2^{(p)}|x|} \tag{104}$$

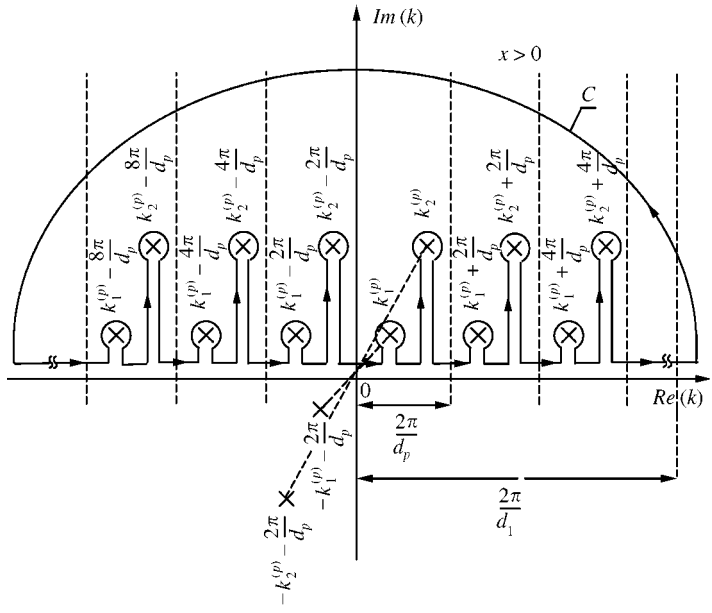

Figure 4. Pictorial representation of the roots of the dispersion relation for a plate with P arrays of attachments.

with the newly defined quantities

$$W_q(x) = \frac{i}{\Phi'(k_q^{(P)})} \sum_{n=-\infty}^{\infty} \Psi(k_q^{(P)} + nk_{d,P})\, \tilde{Y}(k_q^{(P)} + nk_{d,P})\, e^{ink_{d,P}|x|} \quad \text{where } q = 1, 2. \quad (105)$$

We observe that $W_q(x)$ is periodic with the largest array spacing d_P. Thus, each of the two terms in equation (104) satisfies the Floquet theorem cited in the introduction. For comparison to the eigenvalue analysis method, note that the propagation constants are related to the Floquet wavenumbers by

$$\mu_q = ik_q^{(P)} d_P \quad \text{where } q = 1, 2. \quad (106)$$

Thus, $\Re\{(\mu_q)\}$ measures attenuation in the x direction along the plate.

A closed-form expression for the spatial velocity at the cell boundaries, defined as $x = nd_P$ where $n = 0, \pm 1, \pm 2, \ldots$, follows from equation (104),

$$v(nd_P) = W_1(0) e^{ik_1^{(p)}|n|dp} + W_2(0) e^{ik_2^{(p)}|n|dp}. \quad (107)$$

The expressions for the constant $W_{1,2}(0)$ are obtained following the procedure in equations (77)–(82), which yields

$$W_q(0) = \frac{id_P \tilde{Y}_{\Sigma,P}(k_q^{(P)})}{Z_P \tilde{Y}'_{\Sigma,P}(k_q^{(P)})}, \quad \text{where } q = 1, 2 \quad (108)$$

and $\tilde{Y}'_{\Sigma,P}(k) = d\tilde{Y}_{\Sigma,P}(k)/dk$.

The observation that the spatial velocity consists of two wave terms with two different propagation constants agrees with Mead's [14] observation that there are two propagation constants in piecewise periodic structures on flexible supports. Also, it can be shown that

one of the propagation constants is purely negative real with magnitude increasing with frequency. Thus, one of the velocity terms represents a strongly decaying wave that becomes negligible at high frequencies. When the real part of the propagation constant is small, the energy injected through the harmonic force passes freely through the structure with very little attenuation. Those frequency bands for which this is true are known as *pass bands.*

6. EXAMPLE SYSTEM—A THREE-ARRAY STRUCTURE

In this section, the Floquet wavenumbers are evaluated for a three-array structure and compared to finite element predictions computed using Mead's equations [14]. For ease of finite element computations, a beam was modelled instead of a plate. The results derived above are applicable to a beam by replacing the bending rigidity D by $EI/(\rho A)$, replacing the line impedances with point impedances, replacing line forces by point forces, and replacing m by ρA. Recalling Figure 1, the attachments in all arrays were taken as point masses, with each mass equal to the mass of the beam contained within a length d_1. The parameters of the beam were $E = 2 \times 10^{11}$ Pa, $\rho = 7800\ \text{kg/m}^3$, $\nu = 0{\cdot}3$, and $\eta = 0{\cdot}01$. The beam had a square cross-section with thickness $h = 0{\cdot}01$ m.

As a test of the derived dispersion relations, several comparisons were made to numerical calculations based on Mead's equations. To evaluate these equations, a finite element model was developed for one periodic section of the beam. A representative comparison is shown for a three-array structure in Figure 5, which contains a plot of the imaginary part of the Floquet wavenumber of the propagating wave. Differences between the two dispersion curves, which were very small for the considered examples, were attributed to numerical implementation of the two approaches.

A plot of the imaginary parts of the Floquet wavenumbers for the propagating wave is given in Figure 6 for a structure with one, two, and three arrays attached to the beam. This ordering coincides with the sequential ordering of the dispersion given by equations (93)–(95). Large values of the imaginary part indicate high attenuation of a wave along the structure. The real parts of the propagating Floquet wavenumbers in Figure 7 demonstrate that, consistent with one-array structures, the real part of the wavenumber (i.e., the spatial frequency) varies little within the stop bands.

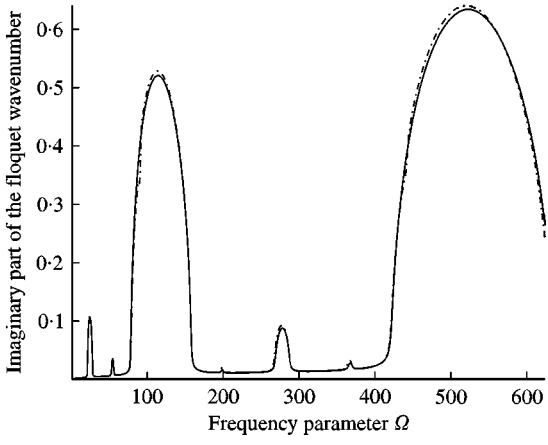

Figure 5. Imaginary part of the propagating Floquet wavenumber, $\Im\{k\}$, versus normalized frequency, Ω, for a beam with three arrays of attachments. The array spacings (in meters) are $d_1 = 1$, $d_2 = 2$, and $d_3 = 4$. Computed from equation (70) - - - -; computed by Mead's equations and a finite element model ——.

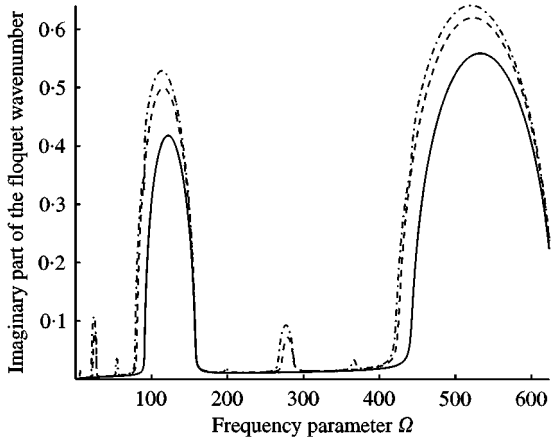

Figure 6. Imaginary part of the propagating Floquet wavenumber, $\Im\{k\}$, versus normalized frequency, Ω, for a beam with one, two, and three arrays of attachments. The array spacings for the three cases (in meters) are $d_1 = 1$; $d_1 = 1$ and $d_2 = 2$; $d_1 = 1$, $d_2 = 2$, and $d_3 = 4$. One array ——; two arrays - - - -; three arrays -·-·-·.

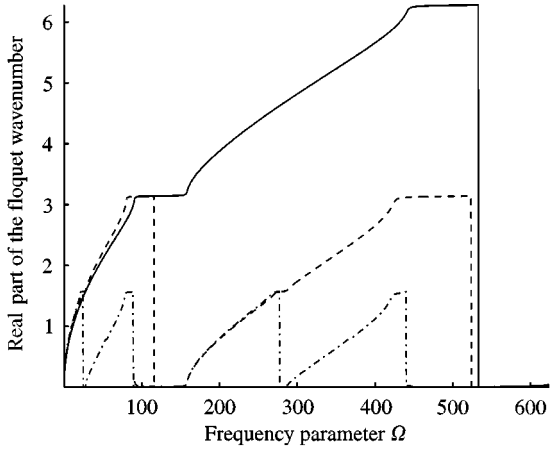

Figure 7. Real part of the propagating Floquet wavenumber $\Re\{k\}$ versus normalized frequency Ω for a beam with one, two, and three arrays of attachments. The array spacings for the three cases (in meters) are $d_1 = 1$; $d_1 = 1$ and $d_2 = 2$; $d_1 = 1$, $d_2 = 2$, and $d_3 = 4$. One array ——; two arrays - - - -; three arrays -·-·-·.

The addition of each array alters the dispersion of the wave in a complex way. To see this, compare Figure 6 with the Floquet wavenumbers of the three corresponding one-array structures plotted in Figure 8. From these figures, it is clear that the stop and pass band features of the individual arrays are not linear (that is, additive). For example, note that the large stop band above $\Omega = 400$ in Figure 6 is very similar to that of the one-array structure with spacing $d = 1$ m shown in Figure 8. For this stop band, the addition of the other arrays has not significantly changed the attenuation. However, the addition of the other arrays does produce smaller stop bands that are visible in Figure 6 near $\Omega = 275$. These stop bands may not be predicted from the corresponding one-array structures in Figure 8.

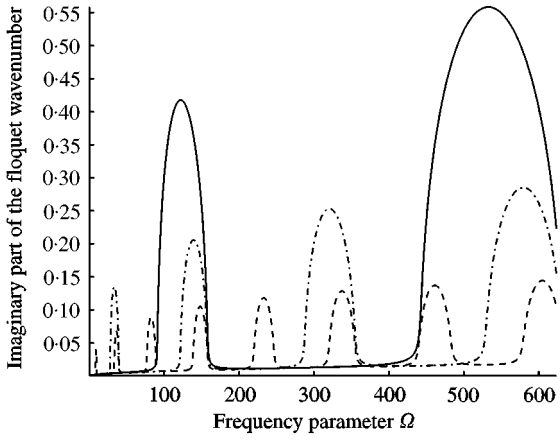

Figure 8. Imaginary part of the propagating Floquet wavenumber, $\Im\{k\}$, versus normalized frequency, Ω, for a beam with one array of attachments. Three array spacings are shown corresponding to $d_1 = 1$, 2, and 4 m. $d = 1$ m ——; $d = 2$ m ·-·-·-·; $d = 4$ m - - - -.

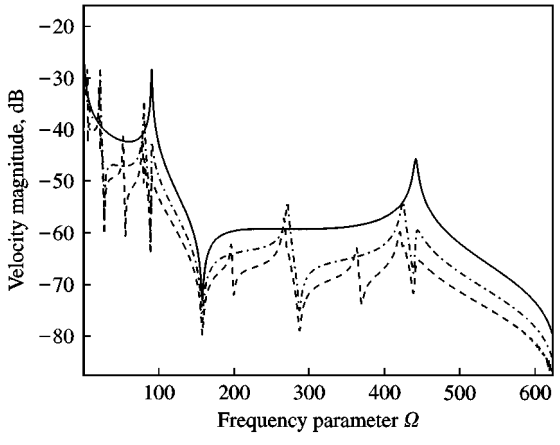

Figure 9. Drive-point velocity magnitude due to the propagating wave versus normalized frequency, Ω, for a beam with one, two, and three arrays of attachments. The array spacings for the three cases (in meters) are $d_1 = 1$; $d_1 = 1$ and $d_2 = 2$; $d_1 = 1$, $d_2 = 2$, and $d_3 = 4$. One array ——; two arrays ·-·-·-·; three arrays - - - -.

In order to understand the effects of stop and pass bands on the velocity at the drive-point ($x = 0$), Figure 9 shows the contribution of the propagating wave to the velocity magnitude for the structures indicated in Figure 8. The velocity maxima occur as the Floquet wavenumber goes through cutoff from a pass band to a stop band. The minima occur as one moves from a stop band to a pass band. Figure 10 depicts the velocity due to the propagating and evanescent waves at two positions away from the drive-point. As anticipated, strong attenuation in the stop bands and weak attenuation in the pass bands correlates with the magnitude of the imaginary part of the propagating Floquet wavenumbers plotted in Figure 8.

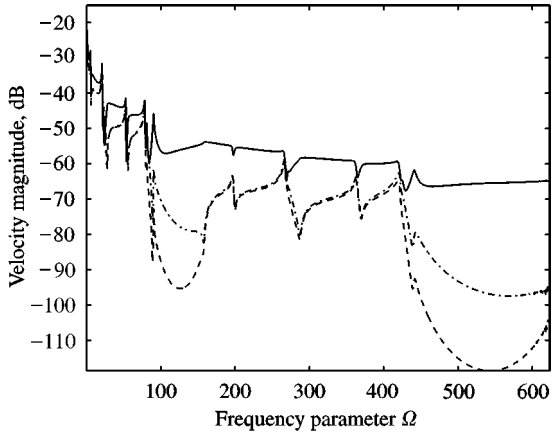

Figure 10. Velocity magnitude due to the propagating and evanescent versus normalized frequency, Ω, for a beam with three arrays of attachments, evaluated at various positions in the structure. At origin ——; At $x = 4$ m -·-·-; At $x = 8$ m - - -.

7. CONCLUSIONS

In contrast to prior work that considered only one- and two-array structures, we have presented a general analytical solution for the wavenumber and spatial velocities of a plate with an arbitrary number of attached arrays. While prior analyses of two–array structures resulted in algebraically complex expressions, one appealing feature of the results presented here is their simplicity. In particular, the Floquet wavenumbers are obtained by analyzing the bare plate first, and then treating the attachment of each array in turn according to their relative spacing. As each array is added to the structure, a quadratic equation is solved for the Floquet wavenumbers.

Another appealing feature of the analysis is its easy extensibility to other geometries and loadings. For example, the analysis could be extended to thin cylindrical shells with arrays of ring attachments by expanding the shell velocities in Fourier series about the circumference of the shell. The Fourier harmonic number would then assume the role of the plate wavenumber k_y in the analysis presented here. The essential steps in the analysis would be repeated and the Floquet wavenumbers $k_p^{(1,2)}$ would describe propagation down the axis of the shell. Similarly, extensions to attachments that apply forces and moments in more than one direction would magnify the algebra but would otherwise be straightforward.

ACKNOWLEDGMENT

The authors gratefully acknowledge the support of the National Science Foundation under Grant Number CMS-9531399. The authors would also like to thank Preston Smith, Jr., whose analyses and insights motivated the present work.

REFERENCES

1. R. H. RACCA 1988 In *Shock and Vibration Handbook*. New York: McGraw-Hill Book Company, Chapter 34, third edition. Types and characteristics of vibration isolators.

2. C. T. Sun & Y. P. Lu 1995 *Vibration Damping of Structural Elements*. Englewood Cliffs, NJ: Prentice-Hall, Chapter 7. Vibrations of constrained damped cylindrical shell structures.
3. J. W. Miles 1956 *Proceedings of the American Society of Civil Engineers, Engineering Mechanics Division*, **EM 1**, 1–9. Vibrations of beams on many supports.
4. L. Brillouin 1946 *Wave Propagation in Periodic Structures, Electric Filters and Crystal Lattices*. New York: Dover Publications, Inc, second edition.
5. Y. K. Lin 1960 *Journal of Applied Mechanics* **27**, 669–676. Free vibration of continuous skin-stringer panels.
6. Y. K. Lin 1962 *International Journal of Mechanical Science* **4**, 409–423. Free vibration of continuous beam on elastic supports.
7. P. W. Smith Jr. 1963 *BBN Technical Report* No. 976. Resonances of a periodically supported beam and its coupling to sound.
8. M. Heckl 1961 *The Journal of the Acoustical Society of America* **33**, 640–651. Wave propagation on beam-plate systems.
9. E. E. Ungar 1961 *The Journal of the Acoustical Society of America* **33**, 633–639. Transmission of plate flexural waves through reinforcing beams; dynamic stress concentrations.
10. E. E. Ungar 1966 *The Journal of the Acoustical Society of America* **39**, 887–894. Steady-state responses of one-dimensional periodic flexural systems.
11. Y. I. Bobrovnitskii & V. P. Maslov 1966 *Soviet Physics Acoustics* **12**, 150–154. Propagation of flexural waves along a beam with periodic point loading.
12. D. J. Mead 1970 *Journal of Sound and Vibration* **11**, 181–197. Free wave propagation in periodically supported, infinite beams.
13. D. J. Mead 1975 *Journal of Sound and Vibration* **40**, 1–18. Wave propagation and natural modes in periodic systems: I. Mono-coupled systems.
14. D. J. Mead 1975 *Journal of Sound and Vibration* **40**, 19–39. Wave propagation and natural modes in periodic systems: II. Multi-coupled systems.
15. D. J. Mead 1973 *Journal of Sound and Vibration* **27**, 235–260. A general theory of harmonic wave propagation in linear periodic systems with multiple coupling.
16. D. J. Mead 1996 *Journal of Sound and Vibration* **190**, 495–524. Wave propagation in continuous periodic structures: research contributions from Southampton, 1964–1995.
17. V. N. Romanov 1971 *Soviet Physics Acoustics* **17**, 92–96. Radiation of sound by an infinite plate with reinforcing beams.
18. V. N. Evseev 1973 *Soviet Physics Acoustics* **19**, 226–229. Sound radiation from an infinite plate with periodic inhomogeneities.
19. M. L. Rumerman 1975 *The Journal of the Acoustical Society of America* **57**, 370–373. Vibration and wave propagation in ribbed plates.
20. G. S. Gupta 1972 *Journal of Sound and Vibration* **20**, 39–49. Propagation of flexural waves in doubly-periodic structures.
21. B. R. Mace 1980 *Journal of Sound and Vibration* **71**, 435–441. Sound radiation from a plate reinforced by two sets of parallel stiffeners.
22. C. B. Burroughs 1984 *The Journal of the Acoustical Society of America* **75**, 714–722. Acoustic radiation from fluid-loaded infinite circular cylinders with doubly periodic ring supports.
23. B. A. Cray 1994 *The Journal of the Acoustical Society of America* **95**, 256–264. Acoustic radiation from periodic and sectionally aperiodic rib-stiffened plates.
24. A. H. Nuttall 1992 *NUWC-NL Technical Report* 10,015, *Naval Undersea Warfare Detachment, New London, Connecticut*. Explicit solution of difference equation for the wavenumber response of fluid-loaded stiffened plate.
25. B. A. Cray 1997 *Fifth International Congress on Sound and Vibration, Adelaide, South Australia*. A formulation for the forced vibration of a multi-supported string.
26. A. Papoulis 1962 *The Fourier Integral and Its Applications. Electronic Science Series*. New York: McGraw-Hill Book Company, Inc.
27. B. R. Mace 1980 *Journal of Sound and Vibration* **73**, 473–486. Periodically stiffened fluid-loaded plates, I. Response to convected harmonic pressure and free wave propagation.
28. L. B. W. Jolley 1925 *Summation of Series*. London: Chapman & Hall, Ltd.